

Analysis and design of nonlinear fiber Bragg gratings and their application for optical compression of reflected pulses

Amir Rosenthal and Moshe Horowitz

Department of Electrical Engineering, Technion-Israel Institute of Technology, Haifa 32000 Israel

Received November 1, 2005; revised January 18, 2006; accepted January 18, 2006; posted February 10, 2006 (Doc. ID 65738)

We demonstrate a novel split-step solution for analyzing nonlinear fiber Bragg gratings. The solution is used for designing nonlinear fiber Bragg gratings with a low reflectivity. The structure of the grating is designed according to the profiles of the incident and reflected pulses. We demonstrate our method for nonlinear compression of a pulse reflected from a fiber Bragg grating. The method allows us to obtain compressed pulses with a very low wing intensity. © 2006 Optical Society of America
OCIS codes: 050.2770, 320.5520.

In recent years, there has been a growing interest in nonlinear phenomena in fiber Bragg gratings (FBGs).¹⁻³ It has been shown that Kerr nonlinearity in FBGs can be used to obtain interesting nonlinear phenomena such as soliton propagation and pulse compression. In Ref. 3 pulse compression was demonstrated in the transmission of an apodized FBG. One of the drawbacks of such an elegant pulse-compression scheme is the residual wings that accompany the compressed pulse, which may limit the use of the compression method for several applications. To minimize the wing intensity and to control the profile of the compressed pulses, a grating structure should be designed. While several design algorithms have been demonstrated for linear gratings,⁴ the problem of designing nonlinear gratings has not been previously studied.

In this Letter we introduce a new split-step solution to the coupled-mode equations, which describe the propagation of pulses in nonlinear FBGs; our solution is accurate, efficient and simple. We used the split-step solution to develop a design method of nonlinear FBGs with a low reflectivity (~25%). We apply our design method to obtain a high-quality pulse compression of the wave reflected from the grating and to give a criterion for the minimum nonlinear effect that is required. Using our method, we obtained a pulse compression with a very weak wing intensity of approximately 0.01% of the maximum pulse intensity. The method can be directly generalized for designing FBGs with a high reflectivity by taking multiple scattering into account.

The propagation of the fields inside the grating is described by the following coupled-mode equations¹:

$$\frac{d}{d\tau} \begin{bmatrix} u(\tau, z) \\ v(\tau, z) \end{bmatrix} = (\mathbf{A} + \mathbf{B}) \begin{bmatrix} u(\tau, z) \\ v(\tau, z) \end{bmatrix}, \quad (1)$$

where

$$\mathbf{A} = \begin{bmatrix} \mathbf{A}_1 & 0 \\ 0 & \mathbf{A}_2 \end{bmatrix}, \quad \mathbf{B} = \begin{bmatrix} 0 & q(z)^* \\ -q(z) & 0 \end{bmatrix}, \quad (2)$$

$$\mathbf{A}_1 = -d/dz + i\Gamma[|u(r, z)|^2 + 2|v(\tau, z)|^2],$$

$$\mathbf{A}_2 = d/dz + i\Gamma[|v(\tau, z)|^2 + 2|u(\tau, z)|^2], \quad (3)$$

where $u(\tau, z)$ and $v(\tau, z)$ are the forward- and the backward-propagating waves, respectively; $\tau = ct/n_{\text{eff}}$ is the normalized time; n_{eff} is the effective refractive index of the fiber; z is the location along the grating; Γ is the nonlinear coefficient; and $q(z)$ is the coupling coefficient of the grating.⁴

We used a split-step method to solve Eq. (1). We divide the grating into N uniform sections, each with a length of Δ . We use the notations for the fields $u_n(\tau_m) = u(\tau = m\Delta, z = n\Delta)$ and $v_n(\tau_m) = v(\tau = m\Delta, z = n\Delta)$ and define the reflectors ρ_n :

$$\rho_n = \sin(|q(n\Delta)|\Delta) \frac{q(n\Delta)}{|q(n\Delta)|} \approx q(n\Delta)\Delta. \quad (4)$$

The propagator $\exp[(\mathbf{A} + \mathbf{B})\Delta]$ is approximated by $\exp(\mathbf{B}\Delta)\exp(\mathbf{A}\Delta)$, where

$$\exp(\mathbf{A}\Delta) \begin{bmatrix} u_n(\tau_m) \\ v_n(\tau_m) \end{bmatrix} = \begin{bmatrix} \exp[i\Gamma\Delta(|u_{n-1}(\tau_m)|^2 + 2|v_n(\tau_m)|^2)]u_{n-1}(\tau_m) \\ \exp[i\Gamma\Delta(|v_{n+1}(\tau_m)|^2 + 2|u_n(\tau_m)|^2)]v_{n+1}(\tau_m) \end{bmatrix} \quad (5)$$

and

$$\exp(\mathbf{B}\Delta) \begin{bmatrix} u_n(\tau_m) \\ v_n(\tau_m) \end{bmatrix} = \begin{bmatrix} \sqrt{1 - |\rho_n|^2} & \rho_n^* \\ -\rho_n & \sqrt{1 - |\rho_n|^2} \end{bmatrix} \begin{bmatrix} u_n(\tau_m) \\ v_n(\tau_m) \end{bmatrix}. \quad (6)$$

Using Eqs. (5) and (6), we obtain the propagation equations

$$\begin{aligned}
 u_n(\tau_{m+1}) &= \sqrt{1 - |\rho_n|^2} u_{n-1}(\tau_m) \exp[i\Gamma\Delta(|u_{n-1}(\tau_m)|^2 \\
 &\quad + 2|v_n(\tau_m)|^2)] \\
 &\quad + \rho_n^* v_{n+1}(\tau_m) \exp[i\Gamma\Delta(|v_{n+1}(\tau_m)|^2 \\
 &\quad + 2|u_n(\tau_m)|^2)], \\
 v_n(\tau_{m+1}) &= \sqrt{1 - |\rho_n|^2} v_{n+1}(\tau_m) \exp[i\Gamma\Delta(|v_{n+1}(\tau_m)|^2 \\
 &\quad + 2|u_n(\tau_m)|^2)] \\
 &\quad - \rho_n u_{n-1}(\tau_m) \exp[i\Gamma\Delta(|u_{n-1}(\tau_m)|^2 \\
 &\quad + 2|v_n(\tau_m)|^2)]. \tag{7}
 \end{aligned}$$

We note that Eqs. (7) give explicit expressions for the propagation of the fields, whereas the numerical solution given in Ref. 5 is based on implicit equations that are solved through iterations, in which each iteration involves approximately five times more operations than do Eqs. (7). To obtain accurate results, we require that the effect of the grating and the nonlinear propagation be small enough in each section of the grating, i.e.,

$$\max_n(|\rho_n|), \quad 2\Gamma \max_{n,m}[|v_n(\tau_m)|^2 + |u_n(\tau_m)|^2]\Delta \ll 1. \tag{8}$$

The conditions in Eq. (8) are fulfilled if Δ is chosen to be small enough.

We demonstrate the accuracy of our split-step solution by analyzing the propagation of a gap soliton. The grating parameters were $q=10^3 \text{ m}^{-1}$ and $\Gamma=5 \text{ W}^{-1} \text{ km}^{-1}$, and the soliton parameters² were $\nu=0.1$ and $\delta=1.5$. The length of each section in the simulation was $\Delta=0.1 \text{ mm}$. Using Eq. (7), we propagated the soliton over 16,000 time points, which corresponds to an effective propagation length of 16 cm. Figure 1 shows the soliton intensity after the propagation, calculated analytically² (the dashed curve) and by using our split-step solution (the solid curve). The maximum difference between the two curves is about 0.8% of the maximum soliton intensity. To obtain the same accuracy, five iterations were needed in the numerical solution given in Ref. 5. Overall, the solution given in Ref. 5 required 25 more operations and had a run time that was 22 times longer than our split-step solution. We also verified our split-step solution for simulating bistable behavior in FBGs and obtained the same results as those reported in Ref. 6.

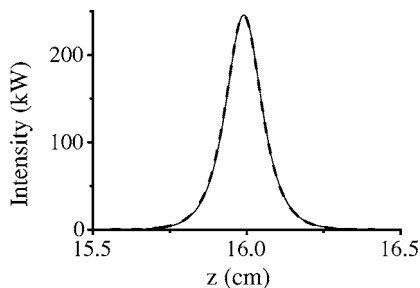


Fig. 1. Intensity of a gap soliton after propagating 16 cm, calculated numerically by using the split-step solution (solid curve) and analytically (Ref. 2) (dashed curve)

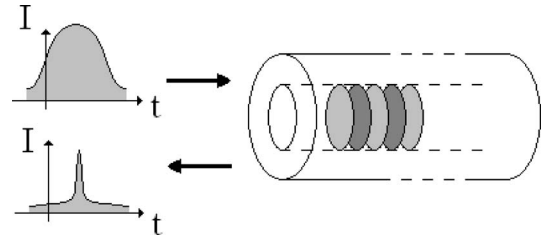


Fig. 2. Schematic description of optical pulse compression geometry.

In a design problem, one needs to find the profile of a grating that gives a desired reflected pulse for a given input pulse (see the schematic in Fig. 2). We restricted our analysis to gratings with weak coupling ($\leq 25\%$ reflectivity). This assumption allowed us to accurately use the Born approximation and to neglect multiple scattering. We also assumed a moderate nonlinear effect and used the undepleted-pump approximation, in which the nonlinear effect of the reflected wave on itself and on the incident wave is ignored.

To obtain the reflected field after a duration of $\tau = m\Delta$, the operators $\exp(\mathbf{B}\Delta)\exp(\mathbf{A}\Delta)$ should be calculated and cascaded m times. When using the Born approximation, we ignored all elements that are on the order of $O(|q|^2)$ or higher and obtained a linear connection between the reflected field and the reflectors:

$$v_1(\tau_{2n-1}) = \sum_{m=1}^n d_{nm} \rho_m, \quad n = 1, 2, 3, \dots, N, \tag{9}$$

where the coefficients d_{nm} are given by

$$\begin{aligned}
 d_{nm} &= u_0(\tau_{2n-2m}) \exp[im\Delta\Gamma|u_0(\tau_{2n-2m})|^2] \\
 &\quad \times \prod_{w=1}^{m-1} \exp[2i\Delta\Gamma|u_0(\tau_{2n-2w-1})|^2]. \tag{10}
 \end{aligned}$$

We define a matrix \mathbf{D} with elements d_{nm} . By inverting the matrix \mathbf{D} we can extract the reflectors ρ_m . In contrast to the linear case ($\Gamma=0$), there are no known criteria for choosing a reflected field that can be realized by a FBG. Our numerical calculations show that when the Kerr effect is not negligible, the matrix \mathbf{D} is ill conditioned.

To overcome the ill conditioning of the matrix \mathbf{D} , we used Tikhonov regularization.⁷ This method stabilizes the problem, since it allows small deviations in the reflected field compared with the desired field. We designate V_{des} as the vector of the desired reflected field at the discrete time values of τ_{2n-1} for $n = 1, 2, 3, \dots, N$. The solution vector that contains the elements of the discrete reflectors ρ_n ($n = 1, 2, 3, \dots, N$) is denoted P . The regularization is obtained by finding the minimum of the functional $\|\mathbf{D}P - V_{\text{des}}\|^2 + \alpha\|P\|^2$, where $\|\cdot\|^2$ denotes the ℓ^2 norm and α is a regularization parameter. The minimum of the functional can be found by setting all its partial derivatives to zero.⁷ $(\mathbf{D}^\dagger\mathbf{D} + \alpha\mathbf{I})P = \mathbf{D}^\dagger V_{\text{des}}$, where \dagger denotes the complex conjugate operation and \mathbf{I} is the identity matrix. The choice of the regularization pa-

parameter α allowed us to control the tradeoff between the accuracy of the reflected field and the amplitude of the reflectors.

We demonstrated our design method for compressing a Gaussian pulse by a compression ratio of $\eta=5$. The incident field is given by $u_0(t)=\sqrt{I_1}\exp[-(t-T_1)^2/\sigma_1^2]$, where $T_1=484$ ps, $\sigma_1=61.2$ ps, and $I_1=10^4$ W. The desired reflected field is given by $v_0(t)=\sqrt{I_2}\exp[-(t-T_2)^2/(\sigma_1/\eta)^2]$. The nonlinear coefficient was chosen to be $\Gamma=6$ W⁻¹ km⁻¹. We chose a maximum intensity of the reflected field, $I_2=900$ W, to ensure a weakly reflecting grating. To obtain a feasible compression, we required that the square root of the second moment of the incident-field spectrum increase during the propagation in the grating by the same amount as the compression ratio, η . In the case of a Gaussian pulse, the second moment of the field spectrum after a propagation of a distance L is given by $\sqrt{\pi/2}I_1/\sigma_1[1+(I_1\Gamma L)^2]$. Using the relation, we obtained the following criterion for the minimum grating length: $\Gamma I_1 L \approx \sqrt{\eta^2-1}$. In our example, we obtained $L=9.5$ cm. Since L corresponds to a time delay of 0.46 ns, we chose $(T_2-T_1)=2 \times 0.46=0.92$ ns.

To avoid boundary effects from the grating ends we chose a grating length of 20 cm. The grating was divided into $N=1000$ sections. Figure 3 shows the phase and the amplitude of the designed grating for three values of the regularization parameter: $\alpha=2 \times 10^2$ (solid curve), $\alpha=2 \times 10^3$ (dashed curve), and $\alpha=2 \times 10^4$ (short-dashed curve). Figure 3 shows that the grating profile remains qualitatively the same for all the values of α . However, as expected, the amplitude of the grating increased as the parameter α decreased.

We verified our design method by calculating the field reflected from the designed grating. Figure 4 shows the desired reflected field (solid curve), compared with the reflected field, calculated for the three grating profiles shown in Fig. 3. Figure 4 shows that the difference between the desired and the calculated pulses increases as α increases. For $\alpha=200$, a very good agreement is obtained between the desired and the calculated reflected fields with a strong wing suppression. The intensity of the wings around the pulse

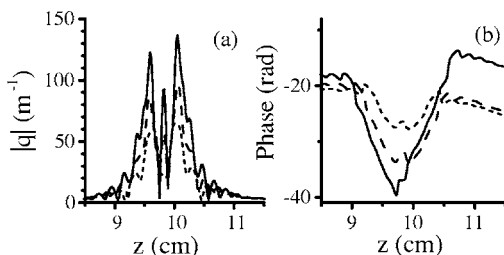


Fig. 3. (a) Amplitude and (b) phase of the designed grating with $\alpha=200$ (solid curve), $\alpha=2000$ (dashed curve), and $\alpha=20,000$ (short-dashed curve).

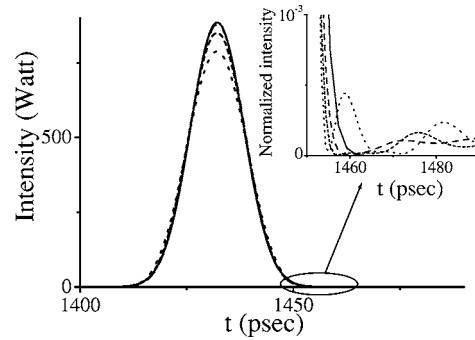


Fig. 4. Desired reflected field (dashed curve) compared with the reflected field, calculated by using a grating designed with $\alpha=200$ (dashed curve), $\alpha=2000$ (short-dashed curve), and $\alpha=20,000$ (dotted curve). The inset shows the wing intensity, normalized to the maximum power of the desired reflected field.

is approximately 4 orders of magnitude smaller than the intensity of the peak. This result is 3 orders of magnitude smaller than that obtained theoretically in Ref. 3.

The compression can be qualitatively understood by comparing the local Bragg wavelength along the grating to the instantaneous frequency change of the incident pulse, caused by the Kerr effect. Figure 3(b) shows that the local Bragg wavelength of the grating is shifted to higher frequencies at the beginning of the grating and to lower frequencies near the end of the grating. Because of the Kerr effect, the leading part of the incident pulse is shifted to lower frequencies, and the end part of the pulse is shifted to higher frequencies. The leading part of the pulse is therefore reflected from the end of the grating, and it experiences a longer time delay compared with the end part of the pulse, which is reflected from the beginning of the grating. The difference in the time delays causes the compression of the reflected pulse.

This work was supported by the Israel Science Foundation (ISF) of the Israeli Academy of Sciences. M. Horowitz's e-mail address is horowitz@ee.technion.ac.il. A. Rosenthal's e-mail address is eeamir@tx.technion.ac.il.

References

1. B. J. Eggleton, C. M. de Sterke, and R. E. Slusher, *J. Opt. Soc. Am. B* **16**, 587 (1999).
2. A. B. Aceves and S. Wabnitz, *Phys. Lett. A* **141**, 37 (1989).
3. J. T. Mok, I. M. Littler, E. Tsoy, and B. J. Eggleton, *Opt. Lett.* **30**, 2457 (2005).
4. A. Rosenthal and M. Horowitz, *IEEE J. Quantum Electron.* **39**, 1018 (2003).
5. C. M. de Sterke, K. R. Jackson, and B. D. Robert, *J. Opt. Soc. Am. B* **8**, 403 (1991).
6. C. M. de Sterke and J. E. Sipe, *Phys. Rev. A* **42**, 2858 (1990).
7. G. H. Golub, P. C. Hansen, and D. P. O'Leary, *SIAM J. Matrix Anal. Appl.* **21**, 185 (1999).